Nordic Hydrolgy, 26, 1995, 125-146

Frost Heave due to Ice Lens Formation in Freezing Soils 1. Theory and Verification

D. Sheng, K. Axelsson and S. Knutsson
Department of Civil Engineering,
Luleå University of Technology, Sweden

A frost heave model which simulates formation of ice lenses is developed for saturated salt-free soils. Quasi-steady state heat and mass flow is considered. Special attention is paid to the transmitted zone, *i.e.* the frozen fringe. The permeability of the frozen fringe is assumed to vary exponentially as a function of temperature. The rates of water flow in the frozen fringe and in the unfrozen soil are assumed to be constant in space but vary with time. The pore water pressure in the frozen fringe is integrated from the Darcy law. The ice pressure in the frozen fringe is determined by the generalized Clapeyron equation. A new ice lens is assumed to form in the frozen fringe when and where the effective stress approaches zero. The neutral stress is determined as a simple function of the unfrozen water content and porosity. The model is implemented on an personal computer. The simulated heave amounts and heaving rates are compared with experimental data, which shows that the model generally gives reasonable estimation.

Introduction

The phenomenon of frost heave has been studied both experimentally and theoretically for decades. Experimental observations suggest that frost heave is caused by ice lensing associated with thermally-induced water migration. Water migration can take place at temperatures below the freezing point, by flowing via the unfrozen water film adsorbed around soil particles. Overburden pressure, temperature gradient and depth to groundwater table are the most important factors that influence frost

heave, Taber (1929, 1930), Penner and Ueda (1977), Penner (1986), Horiguchi (1987) and Konrad (1989).

Theoretically, a number of frost heave models have been proposed, *e.g.* Harlan (1973), Konrad and Morgenstern (1980, 1981, 1982), Gilpin (1980), Hopke (1980), Guymon *et al.* (1980, 1984), O'Neill and Miller (1980, 1985), Shen and Ladanyi (1987) and Padilla and Villeneuve (1992). These models are in general based upon the fundamental principles of thermodynamics and on experimental observations, and have been demonstrated very useful in understanding the phenomenon of frost heave and to some extent also in predicting frost heave for engineering purposes. In respect of

- Adequacy in describing the phenomenon,
- Validation against *e.g.* experimental data,
- Ease in determining input parameters, and
- Applicability in solving practical problems

each of existing models has advantages and disadvantages and very few of them are satisfactory in all the aspects. For instance, the model by O'Neill and Miller (1985) has been considered to be physically elaborate in describing the phenomenon. However, this model has not been validated by any experimental data. In addition, it is difficult to apply this model to solve practical problems which may involve e.g. stratified soil profiles, unsaturated soils, variable ground water table and capillarity, because some parameters needed are rarely available and difficult to determine. On the other hand, the models *e.g.* by Harlan (1973), Guymon *et al.* (1980, 1984) and Konrad and Morgenstern (1980, 1981, 1982) deal with coupled heat and mass transfer in a scale of observation and have been applied to solve field problems. However, an important feature of frost heave, *i.e.* the formation of discrete ice lenses, have not been considered in these models. Detailed review of the existing frost heave models may refer to O'Neill (1982), Berg (1984), Kay and Perfect (1988), Fukuda and Ishizaki (1992) and Sheng (1994).

In an effort to develop a frost heave model which takes into account the basic features of the phenomenon, but which excludes strange parameters, and more importantly which can be further developed into an operational model for solving practical problems, Sheng *et al.* (1992) investigated a model which is somewhat a simplified version of that by Gilpin (1980). The soil was assumed to be saturated and salt-free. Quasi-steady state heat and mass flow was considered and the governing equations were established in a similar manner as by Gilpin (1980). It was assumed that ice lens initiation takes place when and where the maximum ice pressure reaches the total overburden pressure plus the soil tensile strength. A linear variation in the permeability of the frozen fringe was also assumed. The input soil parameters were the dry density, the porosity, the saturated permeability and the thermal conductivity. The heave amounts computed were found very much dependent on the time step and the comparison with the experimental data was not satisfactory.

In this paper, the investigated model will be modified so that a better computational behaviour of the model and a better agreement between the model and experiments will be reached. Modifications are expected to be carried out in many aspects, *e.g.* in the expression of heat and mass equation, in the expression of the neutral stress, in what concerns the criterion for ice lens initiation, and in the permeability and unfrozen water content of the frozen fringe. The modified model will first be presented in this paper in a form of a research model, in order to gain an indepth understanding of the phenomenon, to justify various concepts used in the model and to simulate laboratory tests. In a following paper (this issue), it will be demonstrated that the research model can be further developed into an operational tool which can deal with field conditions such as a stratified soil profile, a varying ground water table, unsaturated soils and snow insulation on the ground surface.

Frozen Fringe and Ice Lens Formation

Freezing of a moist soil is essentially a process coupling heat and mass transfer. When a saturated fine-grained soil is subjected to a subfreezing temperature, part of the water in the soil pores can solidify into ice, *i.e.* pore ice particles; close to soil particles and more tightly bound to them, a film of unfrozen water remains. According to thermodynamics, this adsorbed water film has lower free energy at a lower negative temperature. Therefore a potential gradient can develop along the temperature gradient. Water can be sucked from the warm portion to replace the amount of water lost due to freezing and to feed the accumulation of pore ice. As the pore ice particles grow, they can finally contact each other and form an ice lens, oriented perpendicular to the direction of heat and water flow. In fact, significant frost heave observed in field or laboratory is attributed to ice segregation and ice lens formation associated with water migration.

It is observed that there exists a frozen zone between the growing ice lens and the frost front where the warmest pore ice exists. This zone has been referred to as the frozen fringe, Miller (1977) and Loch and Kay (1978). Within this frozen fringe the temperature drops from the freezing point at the frost front to the segregational temperature at the warm side of the ice lens. In response to this temperature drop, the pore water pressure, unfrozen water content and permeability also decrease through the fringe. The water pressure at the warm side of the lens, which appears in suction, is affected by the segregational temperature and the overburden pressure. Konrad (1989) measured the segregational temperature and pore water pressure in absence of overburden pressure and found they are related to each other by the Clapeyron equation. Unfrozen water content and the permeability decay more or less exponentially with decreasing temperature, Anderson *et al.* (1973), Burt and Williams (1976).

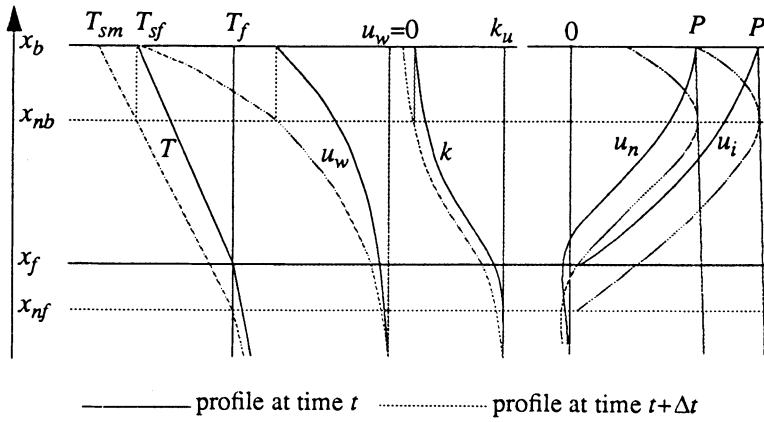

Fig. 1. Mechanisms of ice lens initiation and growth (u_w: water pressure, u_i: ice pressure, u_n: neutral stress, P overburden pressure, P_s separation pressure, T temperature, T_{sf} segregational temperature at ice lens initiation, T_{sm} segregational temperature when the ice lens stops growing, T_f freezing point, k permeability k_u permeability of unfrozen soil, x_b position of current ice lens, x_{nb} position of the new ice lens, x_f position of current frost front, x_{nf} position the frost front at $t+\Delta t$).

As freezing proceeds, the frost front advances in the opposite direction of heat flow, which thickens the frozen fringe. Meanwhile the segregational temperature at the warm side of the growing ice lens drops gradually since the formation of the lens, which results in decreases in the liquid water content and in the permeability of the soil close the ice lens. Therefore, it becomes more and more difficult for water to flow to the warm side of the ice lens. At a certain time, water migration will stop somewhere below the growing ice lens and feed the accumulation of the pore ice at this location. A new ice lens is then initiated.

The criteria governing the ice lens initiation have been studied by a few researchers. Konrad and Morgenstern (1980) stated that the starting position of a ice lens is governed by the local permeability of the current frozen fringe, which is associated with the segregational temperature. As the segregational temperature reaches a critical value, T_{sm}, the permeability is so low that no water is able to flow to the warm side of the growing ice lens. Then a new ice lens appears where the temperature is equal to the initial segregational temperature T_{sf}, Fig. 1. These two segregational temperatures, *i.e.* at the start and the end of a ice lens, are assumed to be constants under specified soil, thermal and overburden conditions. The quantitative determination of T_{sm} and T_{sf} is, however, not known.

Differently from the mechanism of ice lens initiation described above, other researchers have used the concept of the maximum ice pressure or neutral stress. Gilpin (1980) suggested that a new ice lens appears when and where the maximum ice pressure reaches the separation pressure which is equivalent to the overburden pres-

sure plus the soil tensile strength, Fig. 1. In the model by O'Neill and Miller (1980), a neutral stress defined as the difference between the overburden pressure and the effective stress is used instead of the ice pressure. A new ice lens appears when and where the maximum neutral stress reaches the overburden pressure, *i.e.* the effective stress vanishes. The generalized Clapeyron equation is used to relate the water pressure, ice pressure with the temperature within the frozen fringe. The neutral stress is equal to a weighted sum of water and ice pressure. The weight factor depends on the unfrozen water content and porosity. This criterion has advantage in quantitative application and will be employed in this paper. The weight factor in the expression of the neutral stress is, however, evaluated differently from O'Neill and Miller (1985).

Frost Heave Model

Basic Assumptions

Consider a saturated, solute-free soil column subjected to an external distributed load q, as shown in Fig. 2. A subfreezing temperature T_c is applied at the top of the column, whereas the bottom is subjected to a temperature T_w higher than the freezing point of soil water T_f. Both the top and bottom temperatures can vary with time. The external load is, however, assumed to be constant.

Supposing the length of the soil column h and the location of the frozen fringe (x_f, x_b) are known at time level t_n, the aim is to determine the heave rate during a time step Δt and the new location of the fringe at $t_{n+1}=t_n+\Delta t$. With reference to h and (x_f, x_b), the soil column is divided into three zones, *i.e.* frozen zone, frozen fringe and unfrozen zone respectively from top down, Fig. 2. The growing ice lens is included in the frozen zone. During the time period Δt, it is assumed that

- The temperature gradient in each zone is constant,
- The thermal conductivity in each zone is constant,
- The unfrozen water content and the permeability in the unfrozen zone are constant and the unfrozen zone is saturated by capillary or by a water table,
- The permeability of the frozen fringe decreases exponentially as the temperature decreases, and
- The water flows in the frozen fringe and in the unfrozen zone are at steady states.

It should be noted that the assumptions above just hold during a time step but not across the time step. The constant values assumed may vary stepwise. In addition, it is assumed that pore ice particles are always connected with ice lenses as a rigid body. Initiation of a new ice lens takes place when and where the maximum neutral stress within the frozen fringe exceeds the total overburden pressure. The warm end of the soil column is a drainage boundary connected to a constant water table. The x-axis, defining the space coordinate, is directed upwards with the origin at the warm side the soil column.

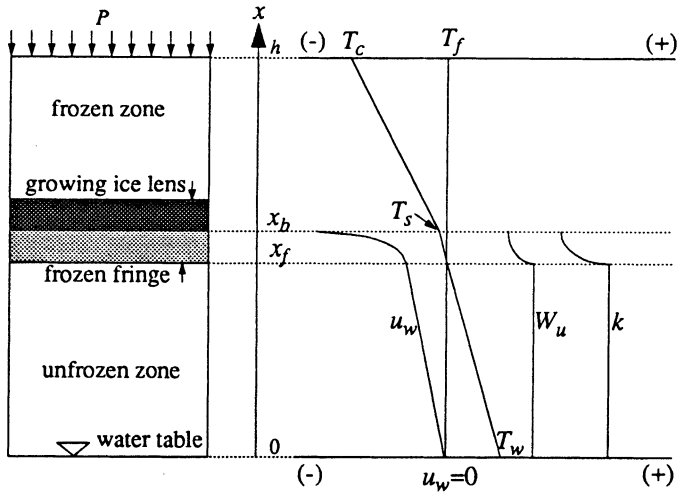

Fig. 2. Temperature, pore water pressure, permeability and unfrozen water content (W_u unfrozen water content by volume).

The assumptions made above, which are expected to reduce the number of parameters that are difficult to determine, will not violate the basic features of the phenomenon of frost heave. For instance, the thermal conductivity is assumed to be constant in space but the permeability is assumed to vary across the frozen fringe. In reality, the both parameters change throughout the frozen fringe due to the change in unfrozen water content. However the variation in the thermal conductivity is in general much less than in the permeability. This can be substantiated by experimental data *e.g.* by Black and Miller (1990) and Horiguchi and Miller (1983). According to Black and Miller (1990), if the unfrozen water content changes, for instance, from 0.5 to 0.25, the permeability will decrease from 10^{-8} to 5×10^{-11} m/s, *i.e.* by a factor 0.005. The data by Horiguchi and Miller (1983) give similar correlations. The increase in thermal conductivity caused by the same change in the unfrozen water content will, however, be less than 1.6 times, if the thermal conductivity is estimated by a geometric mean of the thermal conductivities of the soil phases. This change is small, compared to that in the permeability and therefore not considered in this model.

Heat Balance

In order to establish the heat and mass balance equations, we first study the mass transfer within the frozen fringe. At a time level t_n, we assume that the frozen fringe is located between x_f and x_b, where x_f is the frost front and x_b the warm boundary of the latest ice lens, Fig. 3. Within the fringe, we denote the soil solid fraction by the area filled with thick lines, liquid water by the area filled with thin lines and ice by

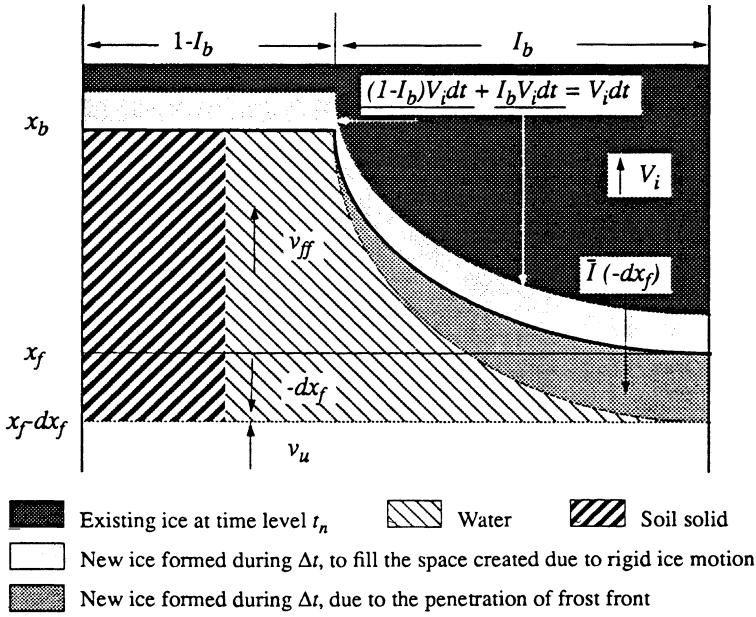

Fig. 3. Schematic view of mass transfer within the frozen fringe.

shaded areas. The volumetric ice content is 1 above x_b, I_b (not necessarily equal 1) at x_b and zero at x_f. Through the fringe it decreases according to the bold curve in the diagram. If the relationship between the unfrozen water content and the temperature is known for the soil under consideration, the shape of the curve is determined uniquely by the segregational temperature at x_b.

If the rigid ice body moves upwards at a velocity V_i, a space of the size ($1\ V_i\ dt$) will be left during time period dt and must be filled by new formed ice. This volume of ice is represented by the lightly shaded area in Fig. 3, which includes the ice formed at x_b, i.e. $I_b\ V_i\ dt$, and that within the fringe, i.e. $(1\text{-}I_b)\ V_i\ dt$. The ice particles within the frozen fringe move upwards through a process referred to as regelation, Miller (1977). In addition, the penetration of the frost front ($-dx_f$) will also cause an ice formation of the volume of $\bar{I}(-dx_f)$, where I is the average ice content in the frozen fringe. This amount of ice is represented by the medianly shaded area in Fig. 3. It should be noted that the same volume of water is reduced in the frozen fringe. Therefore, the total mass in the frozen fringe decreases by $(\rho_w\text{-}\rho_i)\ \bar{I}\ (-dx_f)$.

Now let us consider the heat conservation at the base of the ice lens x_b. The heat flow rate to x_b plus the release rate of latent heat by phase change must equal the rate of heat removal upward through the frozen zone. The rate of latent heat release depends on the amount of ice formed here. The existing ice content has to be subtracted from the total ice content. For a steady thermal state on each side of x_b, the heat balance can be expressed as

$$\lambda_f \frac{T_s - T_c}{h - x_b} - \lambda_{ff} \frac{T_f - T_s}{x_b - x_f} = (1 - I_b) V_i \rho_i L \qquad x = x_b \tag{1}$$

where h is the height of the soil column, λ_f and λ_{ff} are the thermal conductivity of the frozen zone and frozen fringe respectively, L the specific latent heat of water, ρ_i the density of ice, and V_i the rate of ice lens formation or the rate of heave.

Within the frozen fringe, the rate of ice formation is V_i due to rigid ice motion, in addition to $(-dx_f/d_t)\bar{I}$ due to frost front penetration. Therefore, the overall heat balance equation for the frozen fringe can be written as

$$\lambda_f \frac{T_s - T_c}{h - x_b} = \lambda_u \frac{T_w - T_f}{x_f} = \left(V_i - \bar{I} \frac{dx_f}{dt} \right) \rho_i L \qquad x_f \le x \le x_b \tag{2}$$

where λ_u is the thermal conductivity of the unfrozen zone.

Pore Water Pressure and Mass Balance

Since it is assumed that the water flow rate in the frozen fringe, v_{ff}, is a constant, the pore water pressure can then be integrated from the Darcy law

$$v_{ff} = - \frac{k_{ff}}{\rho_w g} \left(\frac{du_w}{dx} + \rho_w g \right) \qquad x_f \le x \le x_b \tag{3}$$

where k_{ff} is the permeability of the frozen fringe, ρ_w the density of water and g the acceleration of gravity. The permeability k_{ff} is assumed to decrease exponentially through the frozen fringe

$$k_{ff} = k_u e^{-b(x - x_f)} \qquad x_f \le x \le x_b \tag{4}$$

where k_u is the permeability of unfrozen saturated soil and b a constant determined in a following section. Substituting Eq. (4) into Eq. (3) and integrating Eq. (3) from x_f to x yields

$$u_w(x) = - v_{ff} \rho_w g \frac{e^{b(x - x_f)}}{b k_u} - \rho_w g x + C \qquad x_f \le x \le x_b \tag{5}$$

where C is an integration constant and can be determined by substituting the boundary value of u_w at x_b. According to the generalized Clapeyron equation, this pore water pressure is related to the segregational temperature T_s and the ice pressure at x_b by, Kay and Groenevelt (1974)

$$\frac{u_w}{\rho_w} - \frac{u_i}{\rho_i} = L \frac{T_s}{T} \qquad x = x_b \tag{6}$$

where T_0 is the freezing point of bulk water in degrees Kelvin, u_i the ice pressure which equals the total overburden pressure. Eliminating the constant C from Eq. (5) by substituting Eq. (6) into Eq. (5) leads to

$$u_w(x) = L\rho_w \frac{T_s}{T} + (q+(h-x_b)\rho_t g)\frac{\rho_w}{\rho_i}$$

$$+ v_{ff}\rho_w g\left(\frac{e^{b(x_b-x_f)} - e^{b(x-x_f)}}{bk_u}\right) + \rho_w g(x_b - x) \qquad (7)$$

where ρ_t is the geometric mean density of frozen soil interlayered with ice lenses.

The mass conservation at x_b requires that the water mass flowing to x_b equals the ice mass formed there

$$v_{ff}\rho_w = (1-I_b)V_i\rho_i \qquad x = x_b \qquad (8)$$

The overall mass balance within the frozen fringe states that the outflow of ice mass at x_b equals the inflow of water mass at x_f plus the decease of mass in the fringe

$$V_i\rho_i = v_u\rho_w + (\rho_w - \rho_i)I\left(-\frac{dx_f}{dt}\right) \qquad x_f \le x \le x_b \qquad (9)$$

The water flow rate in the unfrozen soil, v_u, can be expressed by the Darcy law

$$v_u = -\frac{k_u}{\rho_w g}\left(\frac{u_w(x_f)}{x_f} + \rho_w g\right) \qquad 0 \le x \le x_f \qquad (10)$$

The heat Eqs. (1) and (2), the pore water pressure Eq. (7) and the mass Eqs. (8), (9) and (10) form the basis of the frost heave model. Providing the length of the soil column h and the initial location of the frozen fringe (x_f, x_b) are known, the six equations can be solved for the six unknowns T_s, V_i, dx_f/dt, v_{ff}, v_u and $u_w(x)$. The equation system is non-linear because parameters such as I_b and b are dependent on the temperature T_s. Therefore iteration is needed to solve the system.

Location of the Frozen Fringe

The expression for the neutral stress or the effective pore pressure is proposed by Bishop (1961) for ice-free unsaturated soil. Miller (1977) used the same formula for air-free freezing soil

$$u_n = \chi u_w + (1-\chi)u_i \qquad (11)$$

where χ is a stress partitioning factor and is only a function of the degree of pore saturation, Snyder and Miller (1985). Miller (1977) first approximated χ by w_u/n, *i.e.* the fraction of unfrozen water with respect to the pore space. Hopke (1980) tested

this approximation but found cyclic increases and decreases in the heaving rate. This cyclic behavior of heaving rate was considered unreasonable by Hopke (1980) but observed late by Penner (1986). In O'Neill and Miller's Model, χ was initially set to $(w_u/n)1.5$ (O'Neill and Miller 1980) and then upgraded to an equivalent expression by Snyder and Miller (1985). However, the two different expressions for χ did not lead to any apparent difference in the computed results if we compare the two papers by O'Neill and Miller (1980, 1985), though the authors did not mention this difference. Therefore, we use the simple expression by Miller (1977) for the parameter χ, which results in

$$\sigma = \sigma' + \frac{(n-I)}{n} u_w + \frac{I}{n} u_i = \sigma' + u_n \qquad x_f \leq x \leq x_b \tag{12}$$

where σ denotes the total overburden pressure, σ' the effective stress, u_n the neutral stress, n the soil porosity and I the ice content.

Providing the maximum neutral stress in the frozen fringe governs the initiation of a new ice lens, the aim is to search for the position where the maximum value occurs. Substituting the Clapeyron Eq. (6) to replace the ice pressure u_i in Eq. (12) yields

$$u_n = \left(1 - \frac{I}{n} + \frac{I}{n}\frac{\rho_i}{\rho_w}\right) u_w - \frac{I}{n}\frac{L\rho_i}{T_0} \qquad x_f \leq x \leq x_b \tag{13}$$

Again Eq. (13) is non-linear because of the temperature-dependent ice content I. The derivative du_n/dx is a very complex function of x and the solution $du_n/dx=0$ can not be found easily. In order to find the position of the maximum neutral stress, x_{nb}, we divide the frozen fringe (x_f, x_b) into m equal intervals and compute u_n at each dividing point. The maximum neutral stress and its position can then be determined by interpolation. This maximum value of neutral stress is then compared with the total overburden pressure. If the overburden pressure is exceeded, a new ice lens is assumed to appear at the position x_{nb}. The new frozen fringe is located between x_{bn} and x_f. Otherwise, no new ice lens appears and the position x_b remains during next time step.

So far, the frost heave model is established based upon the knowledge of the initial location of the frozen fringe. The depth of frost penetration during the first time step can be computed approximately by *e.g.* the Neumann solution for pure phase change problems. By assuming an initial segregational temperature, the location of the first ice lens can be determined by interpolation. The initial segregational temperature can be modified after the system of the heat and mass equations have been solved. The location of the first frozen fringe can then be determined by iteration.

Equilibrium Situation

The previous discussion is based on the existence of the frozen fringe. In the case the rate of frost penetration $-dx_f/dt$ is slower than the moving rate of the cold boundary

of the frozen fringe x_b, the frozen fringe will become thinner and thinner. Once the distance between x_b and x_f is too small for computation significance, the frozen fringe is expected to disappear. This is the case when the frost front penetrates close enough to the warm boundary of the soil column. The water flow rate in the unfrozen zone is then in equilibrium with the rate of ice lens formation and thus the frost front will stay still. The heat balance equation becomes

$$\lambda_f \frac{T_s - T_c}{h - x_b} = \lambda_u \frac{T_w - T_s}{x_b} \equiv V_i \rho_i L \tag{14}$$

The Clapeyron Eq. (6) can still be used to determine the pore water pressure at the frost front. The mass balance at the frost front is simplified to

$$V_i \rho_i = v_u \rho_w \tag{15}$$

where v_u is determined by (10). The four Eqs. (6), (10), (14) and (15) can be solved for the four unknowns T_s, V_i, $u_w(x_b)$ and v_u. The soil column is elongated by $(-V_i)\Delta t$ after each time step.

Material Properties

Theoretically all the parameters used in the frost heave model could be treated as input data. This, however, could limit the potential applicability of the model. In order to avoid parameters that are too elaborate to determine, we introduce some empirical relations.

The effective thermal conductivity in the unfrozen zone and the frozen fringe can be computed using the geometric mean

$$\lambda \equiv \lambda_s^{1-n} \lambda_w^{n-I} \lambda_i^{I} \tag{16}$$

where the subscripts s, w and i respectively stand for the soil solid phase, the water phase and the ice phase. The mean value of the volumetric ice content $\bar{I}$ equals zero in the unfrozen zone.

In the frozen zone, frozen soil is interlayered with pure ice lenses. The equivalent thermal conductivity can be calculated in a manner analogous to the resistance in a series electrical circuit, *i.e.*using a harmoic mean

$$\bar{\lambda}_f \equiv \frac{h - x_b}{(h - h_0/\lambda_i) + (h_0 - x_b/\lambda_f)} \tag{17}$$

where λ_f is the thermal conductivity of frozen soil and can be determined by Eq. (16) with $I=n$, and h_o the initial height of the soil column.

The constant b in Eq. (4) can be determined by substituting the permeability at the base of the growing ice lens. The expression suggested by O'Neill and Miller (1985) can be used to calculate this permeability, which gives

$$k_{ff}(x_b) = k_u \left(\frac{W_u(x_b)}{n} \right)^9 = k_u \left(\frac{n-I_b}{n} \right)^9 \tag{18}$$

The volumetric unfrozen water content W_u in the frozen fringe can be expressed as a function of the local temperature or a function of the pore pressure difference (u_w-u_i), Anderson and Tice (1973), O'Neill and Miller (1985), Kujala (1989) and Black and Miller (1990). Alternative relationships have been obtained by regression of experimental data. For instance, that by Black and Miller (1990) states

$$W_u = f(\phi_{iw}) = f(u_i - u_w)$$

where ϕ_{iw} the pressure difference between water and ice. This equation can of course be applied in our model. In fact, by using the Clapeyron equation this formula can also be expressed in terms of temperature. However, the parameters in the formula are not easy to determine and limited experimental data are available.

Another relationship is given by Kujala (1989, 1991)

$$n - I = W_u(T) = W_0 \, e^{\alpha (T)^{\beta}} \tag{19}$$

where W_0 is the initial volumetric water content and α and β parameters dependent on soil specific surface area and pore geometry. This formula is obtained based on 126 laboratory measurements of totally 68 samples covering both coarse and fine finish soils. The parameter β approximately equals 2 for most soils of interest. The parameter α can be determined by substituting the unfrozen water content at a subfreezing temperature *e.g.* -1.0 °C. In the model discussed here, Eq. (19) is applied with β=2.

Computation Strategy

Now we summarize the frost heave model described above. Knowing the following conditions at $t=0$

- Initial height of soil column,
- Soil porosity and dry density,
- Thermal conductivity of soil solid particles,
- Permeability of unfrozen saturated soil,
- Unfrozen water content at a subfreezing temperature, e.g. -1 °C,
- Overburden pressure and initial and boundary temperatures.

We first determine the position the first ice lens according to the theory discussed in the section location of the frozen fringe. The heat and mass balance Eqs. (1) and (2) and Eqs.(7)-(10) are then solved by iteration, for the segregational temperature T_s, the rate of ice lens formation V_i, the rate frost front penetration dx_f/dt, and the pore water pressure $u_w(x)$. The length of the soil column is elongated by $V_i\,\Delta t$. The frost front moves $(-dx_f/dt)\,\Delta t$ downwards. The position of the new frozen fringe is deter-

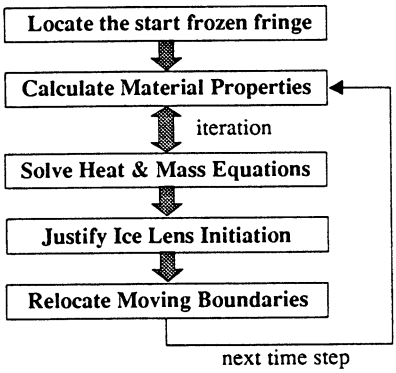

Fig. 4. Flow chart of the frost heave model.

mined according to the ice lens formation criterion described by Eqs. (12)-(13). The system is then ready for next time step. This procedure is illustrated by Fig. 4.

A computer programme for the process described above has been developed and computer graphics has been used to represent heaved soil columns enclosing ice lenses, history diagrams of heave, of frost front, of segregational temperature and of suction in pore water pressure in the frozen fringe. The input parameters include dry density, porosity, saturated permeability, unfrozen water content at a subfreezing temperature, thermal conductivity, boundary temperatures, length of soil column, freezing time and time step for computation.

Experimental Verification

Experimental studies on frost heave have been carried out by many researchers. In this paper, the laboratory results presented by Takeda and Nakano (1990), Penner and Ueda (1977), and Konrad and Morgenstern (1980) are chosen to verify the model presented. The tests by Penner and Ueda are representative for studying the effect of overburden pressures, whereas Konrad and Morgenstern for temperature gradients and Takeda and Nakano for soil types.

Although the test conditions and soil properties are described relatively in detail in these three references, some input parameters needed for simulation are not given. One of them is the unfrozen water content at a subfreezing temperature. If a series of tests on the same sample have been carried out, the parameters needed can be back-estimated using the results from one of the tests and then applied to simulate the others. Otherwise, average values for the soils are used.

Takeda and Nakano (1990)

Freezing tests on three soil samples were conducted using a steady-state method in which the temperature profiles in the soil specimens were controlled. The three soil samples were Kanto loam, Tomakomai silt and Fujinomori clay, with the basic prop-

Table 1 – Soil properties and test conditions of the tests by Takeda and Nakano

Soil sample		Kanto loam	Tomakomai silt	Fujinomori clay
Dry density	kg/m^3	865	1090	1180
Porosity	%	66.3	58.8	55.0
Saturation degree	%	101.7	101.3	96.9
Specific surface area	10^{-3} m^2/kg	191.2	86.2	24.5
Plasticity index	%	15.3	15.1	25.9
Permeability*	10^{-8} m/s	0.20	0.54	0.22
Thermal conductivity	W/mK	0.92	0.93	1.12
Top temperatures	°C	-5.3 ~ -8.6	-2.3 ~ -6.7	-5.3 ~ -6.3
Bottom temperature	°C	8.0	2.0	8.0
Unfrozen/initial water content at -1 °C,%		60	53	45

* Calculated from the given hydraulic conductivity.
† Best fit.

erties listed in Table 1. Two cylindrical soil specimens, 4 cm long and 2.8 cm in diameter, placed parallel to each other in the test cell, were thoroughly insulated so that they freezes unidirectionally from top down. The top and bottom temperatures were adjusted during the tests. No overburden pressure was applied during freezing. Heave and temperature as well as water intake rate were measured.

The simulation of the tests is carried out for a time period 55 hours, with a time step equal to 19.8 seconds. The unfrozen water content at -1 °C is determined so that the measured heave is best fitted. The best fitted value of unfrozen water content is then adjusted with reference to the given specific surface areas. The boundary temperatures used in the simulation are not exactly the same as those in the tests, but the average cooling or heating rate is used.

The computed and measured values of heave are plotted *versus* time in Fig. 5, which shows that a general agreement between the simulated and measured heave exists. It is observed that the model slightly underestimates frost heave for the Kanto loam and the Tomakomai silt, but matches well for the Fujinomori clay.

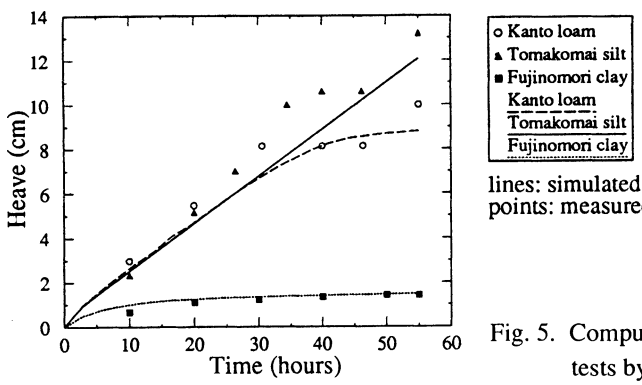

Fig. 5. Computed and measured heave for the tests by Takeda and Nakano.

Table 2 – Soil properties and test conditions of tests by Penner and Ueda

Soil sample		No. 2	No. 4	No. 5	No. 9
Initial water cont. by dry weight	%	16.3	19.5	18.2	23.7
Dry density	kg/m^3	1870	1780	1830	1680
Porosity		0.35	0.35	0.33	0.40
Permeability*	10^{-8} m/s	1.0	0.5	0.1	0.08
Ther. conduc. of soil solid*	W/mK	3.0	3.0	3.0	3.0
Average top temperature	°C	-1.45	-1.75	-0.85	-1.8
Average bottom temperature	°C	2.4	1.9	2.35	1.9
Unfrozen/initial water content † at -1.0 °C	%	36	41	45	53

* Average values.

† Best fit of the measured heave under the lowest overburden pressure.

Table 3 – Computed and measured heave rates for the tests by Penner and Ueda

soil sample	Pressure kPa	Initial length cm	Total heave rate, cm/hour measured	computed	Computed Measured
No. 2	49.0	10.87	1.67×10^{-2}	$*1.67 \times 10^{-2}$	1.00
	98.1	10.66	1.45×10^{-2}	$1.33 \times 1\ 10^{-2}$	0.92
	294.2	10.64	0.42×10^{-2}	0.61×10^{-2}	1.45
	490.3	10.87	0.11×10^{-2}	0.32×10^{-2}	2.91
No. 4	49.0	9.86	2.28×10^{-2}	$*2.29 \times 10^{-2}$	1.00
	147.1	9.4	1.08×10^{-2}	1.63×10^{-2}	1.51
	245.2	9.76	0.51×10^{-2}	0.71×10^{-2}	1.40
	343.2	9.88	0.27×10^{-2}	0.80×10^{-2}	2.96
No. 5	98.1	9.73	1.01×10^{-2}	$*1.01 \times 10^{-2}$	1.00
	196.1	9.97	0.49×10^{-2}	0.67×10^{-2}	1.37
	392.3	9.64	0.26×10^{-2}	0.28×10^{-2}	1.08
	490.3	9.43	0.10×10^{-2}	0.10×10^{-2}	1.00
No. 9	49.0	9.82	3.15×10^{-2}	$*3.15 \times 10^{-2}$	1.00
	147.1	10.15	2.25×10^{-2}	2.28×10^{-2}	1.02
	245.2	10.07	1.59×10^{-2}	1.60×10^{-2}	1.01
	343.2	9.96	0.90×10^{-2}	1.13×10^{-2}	1.26

* Best fit by adjusting the unfrozen water content at -1.0 °C.

Penner and Ueda (1977)

Heaving rates under various overburden pressures were measured in unidirectional freezing tests with constant boundary temperatures. The soils studied include a silty sand *i.e.* No. 2, two silts *i.e.* No. 4 and No. 5, and clayey silt *i.e.* No. 9. The soil samples are all saturated. The physical properties are listed in Table 2. The unfrozen water content at -1 °C, in percentage of the initial water content, is back-estimated from

the measured heave at the lowest overburden pressure for each soil sample and is then used to simulate the tests under higher overburden pressures. The computation is carried out for 60 hours with a time step 21.6 seconds.

The particular values of the computed and measured heaving rates are listed and compared in Table 3, which shows that a general agreement again exists. For the soil samples No. 5 and No. 9, the model gives an excellent estimation of the heaving rate under every pressure. For the samples No. 2 and No. 4, overestimation is observed at some high overburden pressures. A possible reason for the overestimation can be attributed to the way of calculating the heaving rates. In the case of step freezing with constant boundary temperatures, the heaving rate is not constant but decreases gradually as the time increases. The decreasing rate is more pronounced at high pressures. The computed heaving rates are the mean values during the first 60 hours of freezing. The measured heaving rates probably represent a longer period of freezing, though not indicated in the reference.

Table 4 – Computed and measured heave for the tests by Konrad and Morgenstern

Test	T_w, °C	Tc, °C	Initial length cm	Temp. grad. °C/cm	Heave at 60 hours, cm measured†	computed	Computed Measured
NS-1	1.1	-3.4	10.4	0.43	1.24	1.24*	1.00
NS-2	1.1	-4.8	10.4	0.57	1.52	1.53	1.01
NS-4	1.1	-2.5	7.6	0.47	1.32	1.20	0.91
NS-5	1.1	-6.2	10.0	0.73	1.35	1.61	1.19
No.6	1.1	-3.4	6.4	0.70	1.40	1.48	1.06
NS-7	1.1	-3.5	12.0	0.38	1.10	1.17	1.06
NS-9	1.0	-6.0	28.0	0.25	1.00	1.14	1.14
NS-10	1.0	-6.0	18.0	0.39	1.06	1.34	1.26

† Interpolated from Fig. 9 in Konrad and Morgenstern (1980).
* Best fit by adjusting the unfrozen water content at -1.0 °C.

Konrad and Morgenstern (1980)

Konrad and Morgenstern (1980) conducted a series of freezing tests at a constant warm end temperature and under different cold side temperatures. The physical properties of the soil sample Devon silt are as follows: initial water content w_0=33% (Konrad and Morgenstern 1982), saturation S_r=100%, porosity n=0.47, dry density ρ_d=1,440 kg/m^3, and saturated permeability k_s=10^{-9} m/s. The thermal conductivity of soil solid is assumed to be 2.3 W/mK, an average value for most soils. The unfrozen water content at -1 °C is 58% of the initial water content. This value, back-estimated from the measured heave of test NS-1 is consistent with the data (20% by dry weight) given by Konrad (1990). The back-estimated unfrozen water content is then used in simulating other tests.

The computed and the measured values of heave at time 60 hours are listed and compared in Table 4. It is shown that the computed values under low temperature gradients match well the measured data. The heave amounts under large temperature gradients are, however, slightly overestimated.

Summary

A mathematical model for simulation of frost heave and ice lens formation in saturated and salt-free soils has been presented in this paper. Quasi-steady state heat and mass flow has been simulated, with special emphasis on the transmitted zone, the frozen fringe. The permeability of the frozen fringe has been assumed to vary exponentially as a function of temperature. The rates of water flow in the frozen fringe and in the unfrozen soil have been assumed to be constant in space but able to vary with time. The pore water pressure in the frozen fringe has been integrated from the Darcy law. The ice pressure in the frozen fringe has been determined by the generalized Clapeyron equation. A new ice lens has been assumed to form in the frozen fringe when and where the effective stress approaches zero. The neutral stress has been determined as a simple function of the unfrozen water content and porosity. The unfrozen water content in the frozen fringe has been expressed as a function of the temperature.

The frost heave model has been implemented on a personal computer. The input parameters include dry density, porosity, permeability, unfrozen water content, thermal conductivity, external load, boundary temperatures, freezing time and time step. The output results include frost heave, frost penetration, discrete ice lenses, segregational temperature and pore water pressure.

The model has been verified against experimental data by Takeda and Nakano (1990), Penner and Ueda (1977) and Konrad and Morgenstern (1980). The verification has shown that the predicted heave amounts and heaving rates are generally in agreement with the experimental results, although overestimation has been observed under high overburden pressures.

Acknowledgement

The financial support from the Swedish Research Council for Engineering Science (TFR) is appreciated.

Notations

g	Acceleration of gravity	m/s^2
h	Length of soil column	m
I	Ice content	
I_b	Ice content at the base of the growing ice lens	
$\bar{I}$	Mean ice content in the frozen fringe	
k	Permeability	m/s
k_{ff}	Permeability of the frozen fringe	m/s
k_u	Saturated permeability of unfrozen soil	m/s
L	Specific latent heat of water	J/kg
n	Porosity of soil	
q	Overburden pressure	Pa
t	Time	s
Δt	Time step	s
T	Temperature	°C
T_c	Applied temperature at the cold side	°C
T_f	Freezing temperature soil moisture	°C
T_o	Freezing point of bulk water	degree Kelvin
T_s	Segregational temperature	°C
T_{sf}	Segregational temperature at the start of a ice lens	°C
T_{sm}	Segregational temperature at the end of a ice lens	°C
T_w	Applied temperature at the warm side	°C
u_i	Ice pressure	Pa
u_n	Neutral stress	Pa
u_w	Pore water pressure	Pa
v_{ff}	Rate of water flow in the frozen fringe	m/s
v_u	Rate of water flow in the unfrozen soil	m/s
V_i	Rate of ice lensing (rate of heave)	m/s
W_u	Unfrozen water content by volume	
w_u	Unfrozen water content by dry weight	
x_b	Base position of the growing ice lens	m
x_f	Position of frost front (0-isotherm)	m
x_{nb}	Base position of the new ice lens	m
x_{nf}	Position of the new frost front	m
λ_f	Thermal conductivity of frozen soil	W/(m°C)
λ_f	Effective thermal conductivity of frozen soil with ice lenses	W/(m°C)
λ_{ff}	Thermal conductivity of frozen fringe	W/(m°C)
λ_i	Thermal conductivity of ice	W/(m°C)
λ_s	Thermal conductivity of soil solid	W/(m°C)
λ_u	Thermal conductivity of unfrozen soil	W/(m°C)
λ_w	Thermal conductivity of water	W/(m°C)
ρ_t	Total density of frozen soil	kg/m^3
ρ_i	Density of ice	kg/m^3
ρ_w	Density of water	kg/m^3
σ'	Effective stress	Pa
χ	Stress partitioning factor	

References

Anderson, D. M., and Tice, A. R. (1973) The unfrozen interfacial phase in frozen soil-water systems, *Ecological Studies*, Springer Verlag, *Vol. 4*, pp. 107-124.

Berg, R. L. (1984) Status of numerical models for heat and mass transfer in frost-susceptible soils, 4 th Int. Conf. Permafrost, Final Proc., National Academy Press, Washington, D.C., pp. 67-71.

Black, P. B., and Miller, R. D. (1985) A continuum approach to modelling of frost heaving. In Freezing and Thawing of Soil-Water Systems (D. M. Anderson and P. J. Williams, eds.) Technical Council on Cold Regions Engineering Monograph, ASCE, pp. 36-43.

Black, P. B., and Miller, R. D. (1990) Hydraulic conductivity and unfrozen water content of air-free frozen silt, *Water Resour. Res., Vol. 26, No. 2*, pp. 323-329.

Burt, T. P., and Williams, P. J. (1976) Hydraulic conductivity in frozen soils, *Earth Surface Processes, Vol. 1*, pp. 349-360.

Eigenbrod, KD, Knutsson, S., and Sheng, D. (1991) Measurement of pore pressures in freezing and thawing soft fine-grained soils, Proc. of 44 th. Can. Geotech. Conf., Winnipeg, Canada Geotechnical Society.

Farouki, O. T. (1986) *Thermal properties of soils*, Clausthal-Zellerfeld, Trans Tech Publication.

Fukuda, M., and Ishizaki, T. (1992) General report on heat and mass transfer, Proc. 6th Int. Symp. Ground Freezing, Balkema, Rotterdam, Vol. 2, pp. 409-416.

Gilpin, R. R. (1980) A model for the prediction of ice lensing and frost heave in soils, *Water Resour. Res., Vol. 16, No. 5*, pp. 918-930.

Groenevelt, P. H., and Kay, B. D. (1974) On the interaction of water and heat transport in frozen and unfrozen soils: i. basic theory; the liquid phase, *Soil Sci. Soc. Amer. Proc., Vol. 38*, pp. 400-404.

Guymon, G. L., Hromadka II, T. V., and Berg, R. L. (1980) A one-dimensional frost heave model based upon simulation of simultaneous heat and water flux, *Cold Reg. Sci. Technol., Vol. 3*, pp. 253-262.

Guymon, G. L., Hromadka II, T. V., and Berg, R. L. (1984) Two-dimensional model of coupled heat and moisture transport in frost-heaving soils, *J. Energy Resour. Technol., Vol. 106, No. 3*, pp. 336-343.

Harlan, R. L. (1973) Analysis of coupled heat and mass transfer in partial frozen soil, *Water Resour. Res., Vol. 9, No. 5*, pp. 1314-1323.

Holden, J. T., Piper, D., and Jones, R. H. (1985) Some development of a rigid-ice model of frost heave, Proc. 4th Int. Symp. Ground Freezing, Balkema, Rotterdam, pp. 93-98.

Hopke, S. (1980) A model for frost heave including overburden, *Cold Reg. Sci. Technol., Vol. 3*, pp. 111-127.

Horiguchi, K. (1987) Effect of cooling rate on freezing of saturated soil, *Cold Reg. Sci. Technol., Vol. 14*, pp. 147-153.

Horiguchi, K., and Miller, R. D. (1983) Hydraulic conductivity functions of frozen materials, Proc. 4th Int. Conf. Permafrost, National Academy Press, Washington, D.C., pp. 504-508.

Jame, Y. W., and Norum, D. I. (1980) Heat and mass transfer in a freezing unsaturated porous medium, *Water Resour. Res., Vol. 16*, pp. 811-819.

Jansson, P.-E., and Halldin, S. (1979) Model for the annual water and energy flow in a layered soil, *Comparison of frost and energy models* (S. Halldin, ed), Soc. Ecol. Modelling, Copen-

hagen, pp. 145-163.

Kay, B. D., and Groenevelt, P. H. (1974) On the interaction of water and heat transport in frozen and unfrozen soils: i. basic theory; the vapor phase, *Soil Sci. Soc. Amer. Proc., Vol. 38*, pp. 395-400.

Kay, B. D., and Perfect, E. (1988) State of the art: heat and mass transfer in freezing soils, Proc. 5th Int. Symp. Ground Freezing, Balkema, Rotterdam, pp. 581-596.

Knutsson, S., Domaschuk, L., and Chandler, N. (1985) Analysis of large scale laboratory and in situ frost heave tests, Proc. 4th Int. Symp. Ground Freezing, Balkema, Rotterdam, pp. 65-70.

Konrad, J. M., and Morgenstern, N. R. (1980) A mechanistic theory of ice lens formation in fine-grained foils, *Can. Geotech. J., Vol. 17*, pp. 473-486.

Konrad, J. M., and Morgenstern, N. R. (1981) Segregational potential of freezing soil, *Can. Geotech. J., Vol. 18*, pp. 482-491.

Konrad, J. M., and Morgenstern, N. R. (1982) Effect of freezing pressure on freezing soils, *Can. Geotech. J., Vol. 19*, pp. 494-505.

Konrad, J. M. (1989) Influence of cooling rate on the temperature of ice lens formation in clayey silts, *Cold Reg. Sci. Technol., Vol. 16*, pp. 25-36.

Kujala, K. (1989) Unfrozen water content of Finish soils measured by NMR, Proc. Int. Symp. on Frost in Geotechnical Engineering (H. Rathmayer, ed.), Espoo, Technical Research Centre of Finland, Vol. 1, pp. 301-310.

Kujala, K. (1991) Factors affecting frost susceptibility and heaving pressure in soils, Ph. D. Dissertation, University of Oulu, Finland.

Loch, J., and Kay, B. D. (1978) Water redistribution in partially frozen, saturated silt under several temperature gradients and overburden loads, *Soil Sci. Soc. Amer. Proc, vol. 42*, pp. 400-406.

Lundin, L.-C. (1989) Water and heat flows in frozen Soils, Doctoral dissertation, Uppsala University, Uppsala.

Miller, R. D. (1977) Lens initiation in secondary heaving, Int. Symp. on Frost Action in Soils, Luleå University of Technology, Sweden, Vol. 2. pp. 68-74.

Miller, R. D. (1980) Freezing phenomena in soils. In *Application of Soil Physics* (D. Hillel, ed), Academic Press, pp. 254-299.

Nixon, J. F. (1992) Discrete ice lens theory for frost heave beneath pipelines, *Can. Geotech. J., Vol. 29*, pp. 487-497.

O'Neill, K., and Miller, R. D. (1980) Numerical solutions for rigid-ice model of secondary frost heave, Proc. 2nd Int. Symp. Ground Freezing, Trondheim, The Norwegian Institute of Technology, Vol. 1, pp. 656-669.

O'Neill, K. (1983) The physics of mathematical frost heave models: a, review, *Cold Reg. Sci. Technol., Vol. 6*, pp. 275-291.

O'Neill, K., and R. D. Miller (1985), Exploration of a rigid -ice model of frost heave, *Water Resour. Res., Vol. 21, 3*, pp. 281-296.

Padilla, F., and Villeneuve, J. P. (1992) Modeling and experimental studies of frost heave including solute effects, *Cold Reg. Sci. Technol., Vol. 20*, pp. 183-194.

Penner, E. (1986) Aspects of ice lens growth in soils, *Cold Reg. Sci. Technol., Vol. 13*, pp. 91-100.

Penner, E., and Ueda, T. (1977) The dependence of frost heaving on load application – preliminary results, Int. Symp. on Frost Action in Soils, Luleå University of Technology,

Sweden, Vol. 1, pp. 137-142.

Shen, M., and Ladanyi, B. (1987) Modelling of coupled heat, moisture and stress field in freezing soil, *Cold Reg. Sci. Technol., Vol. 61*, pp. 417-429.

Sheng, D. (1994) Thermodynamics of freezing soils, theory and application, Doctoral Dissertation, 1994:141D, Luleå University of Technology.

Sheng, D., Knutsson, S., and Eigenbrod, D. (1992) Test and simulation of frost heave, 11th Nordic Geotechnical Meeting, Danish Geotechnical Society, Vol. 2, pp. 485-490.

Sheng, D., Axelsson, K., and Knutsson, S. (1993) Finite element analysis for convective heat diffusion with phase change, *Comp. Meth. Appl. Mech. Eng., Vol. 104*, pp. 19-30.

Sheng, D., Axelsson, K., and Knutsson, S. (1995) Frost Heave due to Ice Lens Formation in Freezing soils, 2. Filed Application, *Nordic Hydrology, Vol. 26* (2) pp. 147-168.

Sheng, D., and Knutsson, S. (1993) Sensitivity analysis of frost heave – A theoretical study, Proc. 2nd Int. Symp. on Frost in Geotechnical Engineering (A. Phukan,ed.), Balkema, Rotterdam, pp. 3-16.

Snyder, V. A., and Miller, R. D. (1985) Tensile strength of unsaturated soils, *Soil Sci. Soc. Am. J., Vol. 49*, pp. 58-65.

Taber, S. (1929) Frost heaving, *J. Geol., Vol. 37*, pp. 428-461.

Taber, S. (1930) The mechanics of frost heaving, *J. Geol., Vol. 38*, pp. 303-317.

Taylor, G. S., and Luthin, J. N. (1978) A model for coupled heat and moisture transfer during soil freezing, *Can. Geotech. J., Vol. 15*, pp. 548-555.

First received: 4 July, 1994
Revised version received: 10 September, 1994
Accepted: 26 September, 1994

Address:
Department of Civil Engineering,
Luleå University of Technology,
S-971 87 Luleå,
Sweden.